Fission and binary fragmentation reactions in Se-80+Pb-208 and Se-80+Th-232 systems

Fission and binary fragmentation reactions in ^{80}Se+^{208}Pb and ^{80}Se+^{232}Th systems

R. G. Thomas,[1] A. Saxena,[1] P. K. Sahu,[1] R. K. Choudhury,[1,2] I. M. Govil,[3] S. Kailas,[1] S. S. Kapoor,[1] M. Barbui,[4] M. Cinausero,[4] G. Prete,[4] V. Rizzi,[4] D. Fabris,[5] M. Lunardon,[5] S. Moretto,[5] G.Viesti,[5] G. Nebbia,[5] S. Pesente,[5] B. Dalena,[6] G. D'Erasmo,[6] E. M. Fiore,[6] M. Palomba,[6] A. Pantaleo,[6] V. Paticchio,[6] G. Simonetti,[6] N. Gelli,[7] and F. Lucarelli[7]

[1]*Nuclear Physics Division, Bhabha Atomic Research Centre, Mumbai 400085, India*

[2]*Institute of Physics, Bhubaneswar 751005, India*

[3]*Department of Physics, Punjab University, Chandigarh 160014, India*

[4]*INFN Laboratori Nazionali di Legnaro, I-35020 Legnaro (Pd), Italy*

[5]*Dipartimento di Fisica and Sezione INFN Padova, I-35131 Padova, Italy*

[6]*Dipartimento Interuniversitario di Fisica and Sezione INFN Bari, I-70100 Bari, Italy*

[7]*Dipartimento di Fisica and Sezione INFN Firenze, I-50125 Firenze, Italy*

(Received 2 May 2006; published 12 February 2007)

Fission and binary fragmentation of the excited nuclear systems of $Z = 116$ and 124 were investigated using the reactions induced by ^{80}Se beams on ^{208}Pb and ^{232}Th targets at bombarding energies ranging from 470 to 630 MeV. The mass and kinetic energy of the binary reaction products were reconstructed by measuring their velocities by the time-of-flight method and the angles of emission using multiwire proportional chambers. Total neutron multiplicities were measured in coincidence with the fragments, using an array of neutron detectors. The fragment mass-energy correlation was studied for the two systems. The average total kinetic energy (TKE) of fragments for the ^{80}Se+^{208}Pb system agrees with earlier measurements and with Viola's systematics in the mass symmetric region for compound nucleus fission, whereas for the ^{80}Se+^{232}Th system, the TKE values are significantly lower. This is also consistent with higher values of total neutron multiplicities observed for the case of ^{80}Se+^{232}Th at comparable available energies. From an extrapolation of the measured total neutron multiplicities for the mass symmetric region to zero compound nucleus excitation energy, the average number of prompt neutrons expected to be emitted in the spontaneous fission of the superheavy $Z = 116$ has been estimated to be $\nu_{\rm tot}^{\rm sf} = 10 \pm 2$, which is consistent with the value derived for the same compound nucleus populated in the ^{56}Fe+^{232}Th reaction in an earlier work. In the case of the ^{80}Se+^{232}Th system, similar analysis was carried out by taking the average TKE from Viola's systematics for estimating the available energy for particle emission corresponding to compound nucleus fission. In this way, by extrapolating the observed neutron multiplicities to zero compound nucleus excitation energy, a value of $\nu_{\rm tot}^{\rm sf} = 15 \pm 2$ was obtained for the spontaneous fission of the superheavy $Z = 124$ nucleus. The increase in the average number of neutrons emitted in fission as a function of the atomic number of the nucleus in the superheavy mass region was confirmed by comparing the results of the present work with published data.

DOI: 10.1103/PhysRevC.75.024604 PACS number(s): 25.70.Jj

I. INTRODUCTION

Recently, there has been a great deal of interest in the study of binary fragmentation of superheavy composite systems formed in heavy-ion reactions using different entrance channels. The formation of a superheavy compound nucleus and its subsequent deexcitation by particle emission resulting in an evaporation residue of the superheavy nucleus depends on a number of factors [1–5]. The production cross section of a superheavy nucleus as an evaporation residue (ER) can be written as

$$\sigma_{\rm ER} = \sigma_{\rm CAP} P_{\rm CN} (1 - P_f), \tag{1}$$

where $\sigma_{\rm CAP}$ is the cross section for capture toward fusion of the two colliding heavy ions, $P_{\rm CN}$ is the probability that after capture, the dinucleus results in the formation of a compound nucleus (CN), and P_f is the cumulative probability for the CN to decay by fission during the deexcitation cascade. The study of binary fragmentation is relevant for ascertaining the optimum conditions to maximize the cross section for the first step toward the formation of a superheavy compound nucleus and for the study of its fission characteristics [6–8].

It is well known that in heavy-ion reactions, competing non-compound-nucleus fission (NCNF) channels—such as quasifission, fast-fission, and preequilibrium-fission mechanisms, generally grouped together as quasifission (QF)—hinder the formation of a compound nucleus [9–16]. The probability of these quasifission processes depends strongly on the entrance channel parameters, viz. the bombarding energy, mass asymmetry, and deformation of the colliding nuclei. Swiatecki *et al.* [10,11] have discussed the heavy-ion fusion process in terms of the three "milestone configurations" of the colliding system: the touching configuration, conditional saddle point at frozen mass asymmetry, and unconditional saddle-point configuration. It is pointed out that a threshold energy called extra-extra-push energy is required to cross over the unconditional saddle point to reach the fusion valley, and this energy depends on the entrance channel mass asymmetry. But when this additional energy is imparted, the system is also formed in a higher excited state and therefore has less chance of survival against fission, leading to a reduction in the

probability for formation of the evaporation residue. In a recent work by Swiatecki *et al.* [12], the above static picture [10,11] was modified by considering the dynamical factor of diffusion to account for the probability of the composite system reaching the compound nucleus configuration by thermal fluctuations even when the system is formed below the barrier. Moller and Sierk [13] discussed the role played by the microscopic degrees of freedom to also include nuclear shell effects in deciding the reaction paths leading to the fusion and nonfusion processes. It is, thus, important to experimentally investigate the various factors that come into play in the formation of the CN and subsequently the evaporation residue, in order to determine the optimum conditions for which the product of the three factors in Eq. (1) is maximized [14–17]. The present study is aimed toward understanding the dynamics of fusion as well as decay of the superheavy fused composite system on its way to compound nucleus formation and its dependence on the entrance channel mass asymmetry and bombarding energy. Earlier studies of binary fragmentation have been reported by Itkis *et al.* [6,7,18] for a number of target-projectile systems at low bombarding energies leading to superheavy composite systems. Their work investigated the mass-energy distributions as well as neutron and γ emission characteristics in the fission of $Z = 102$–122 nuclei populated in various entrance channels. It is of interest to extend such studies of fusion dynamics and the fission mechanism in the superheavy mass region to higher bombarding energies and heavier systems.

We have pursued a program in this direction and carried out studies of the binary fragmentation of superheavy composite nuclear systems through measurements of the velocity vectors of the two outgoing fragments. Neutrons emitted in coincidence with the fragments have also been measured in order to understand the energetics of the binary fragmentation process. In an earlier work, we reported [19] the results for the case of the ^{56}Fe+^{232}Th system at 372 MeV bombarding energy where it has been shown that most of the binary fragmentation events in the near-symmetric mass splits appear to arise from mass-asymmetric fission of the compound nucleus. There was also an indication of the influence of $Z = 50$ and $N = 82$ shells of the light fragment group of the mass distribution of the binary fragments. The average pre-scission and total neutron multiplicities were determined from the mass-energy correlations measured with and without neutron coincidence. By extrapolating the neutron emission data to zero compound nucleus excitation energy, it was possible to deduce the average neutron multiplicity, $\nu_{\rm tot}^{\rm sf}$, that should correspond to the case of spontaneous fission of the superheavy nucleus $_{116}$X^{288}. This neutron multiplicity was estimated to be $\nu_{\rm tot}^{\rm sf} \sim 12 \pm 1$.

In the present study, we have extended the measurements of the fragment mass and kinetic energy correlations and neutron multiplicities to the ^{80}Se+^{208}Pb and ^{80}Se+^{232}Th systems. The former reaction leads to the same composite system, $_{116}$X^{288} studied in the previous ^{56}Fe-induced reaction, through a more symmetric entrance channel. The ^{80}Se+^{232}Th reaction populates a much heavier superheavy system, not investigated so far. The experiments were carried out at different bombarding energies of the ^{80}Se beam on both the targets, thus exploring the bombarding energy dependence of the binary fragment mass yields, mass–kinetic-energy correlations, and total neutron multiplicities. From these data, we have also deduced the information on the neutron yields from the fragments corresponding to the fission of the superheavy nuclei of $(Z, A) = (116, 288)$ and $(124, 312)$ at zero excitation energy. The details of the experimental setup and data analysis are described in Secs. II and III, respectively. The results are discussed in Sec. IV. Section V contains the summary and conclusions of the present studies.

II. EXPERIMENTAL DETAILS

The experiments described in this work were performed using the ^{80}Se beams from the tandem ALPI heavy-ion accelerator facility of the Laboratori Nazionali di Legnaro, Italy. The experimental setup was similar to the one used in the earlier measurements for the ^{56}Fe+^{232}Th system, as described in Ref. [19]. In the following, the key features of the experimental setup are briefly presented.

The ^{80}Se beam with an intensity of 0.5–1 pnA delivered by the tandem XTU-ALPI superconducting linear accelerator complex was focused onto self-supporting ^{208}Pb and ^{232}Th targets having thicknesses of 400 μg/cm^2 and 1.5 mg/cm^2, respectively. The experiment was carried out at bombarding energies ranging from 470 to 630 MeV for both systems. The targets were located at the center of a thin-walled (3 mm) spherical aluminum scattering chamber of 100 cm diameter. A schematic view of the experimental setup used in this work is shown in Fig. 1. The heavy reaction products were detected in two time-of-flight (TOF) arms. One TOF arm consisted of a 2 cm diameter microchannel plate (MCP) detector placed at a distance of 7 cm from the target followed by a large-area (13.5 × 13.5 cm^2) position-sensitive multiwire proportional counter (MWPC1) with a resulting opening angle $\Delta\theta_{\rm lab} = \pm 8^\circ$. The flight path between the MCP and MWPC1

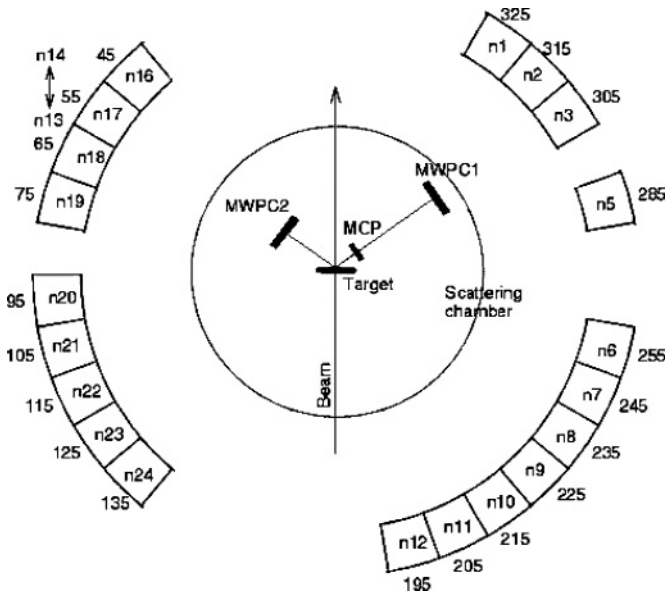

FIG. 1. Schematic view of experimental setup. The angles of the neutron detectors with respect to the beam direction are marked outside the boxes.

was 26 cm. The MCP was used to provide the start signal to measure the TOF in both arms. This TOF arm was positioned at $\theta_{\rm lab} = 55^\circ$, which is behind the reaction grazing angle for both systems. The second TOF arm consisting of another large area (13.5×13.5 cm^2) position-sensitive multiwire proportional counter (MWPC2) was placed at a distance of 17 cm from the target on the opposite side of the first arm with respect to the beam and centered at $\theta_{\rm lab} = 55^\circ$ with an opening angle of $\pm 16^\circ$. The acceptance of the TOF arms allows the detection of coincident pairs of fragments from elastic scattering as well as from symmetric and asymmetric fragmentation of the composite system.

Neutrons were detected in 22 BC501 liquid scintillator cells, each of 12.5 cm diameter and 12.5 cm thickness. Neutron detectors were placed around the scattering chamber at a distance of 2 m from the target, for measuring the neutron TOF with respect to the MCP start signal. The absolute neutron TOF was determined using the γ-ray peak in the TOF spectrum as reference.

The trigger of the data acquisition was generated by a logic OR signal of suitably prescaled fragment singles (defined as MCP-MWPC1 coincidences), binary fragment events (defined as MCP-MWPC1-MWPC2 coincidences), and triple coincidence events (defined by the coincidence of two-fragment events with any of the neutron detectors). The data analysis was carried out using software tools based on the ROOT package as in our earlier works [19–21].

III. DATA ANALYSIS

The data were analyzed to obtain various distributions and correlations of the two-fragment events in the exit channel of the reaction with and without coincidence with the neutron detectors. The polar angle θ and the azimuthal angle ϕ of the MWPCs were calibrated using the image of the edges of the detectors in the position spectra and the known position of the entrance window support wires. At the lowest bombarding energy, i.e., 470 MeV, the grazing angle was larger than $\theta_{\rm lab} = 50^\circ$, thus allowing the elastically scattered events to enter inside the first TOF arm. The calibration of the time spectrum of fragment detectors was achieved using the elastic scattering peak at 50° for both systems.

The velocity vectors of the fragments were constructed using the TOF and the position information (θ and ϕ) Proper corrections were applied for the energy loss of fragments in the target and the Mylar foil (1.5 μm thick) of the MCP. The offset in the start signal due to the transit time of fragments entering the MCP was properly taken into account in determining the time of flight of the fragments. The measured laboratory velocities of the fragments were converted into center-of-mass velocities by applying kinematic transformations assuming a two-body exit channel. The provisional fragment masses were obtained by applying the usual linear momentum and mass conservation relationships. Starting with the provisional masses, an iterative procedure was adopted incorporating all the above corrections to determine the fragment masses and kinetic energies using the measured TOF values of the fragments. The iteration process was repeated to ensure convergence of the final fragment masses and kinetic energies.

In the present study, we analyzed only that class of events in which the lighter fragment, ranging from the projectile mass $A_p = 80$ to $A_{\rm FFL} = (A_p + A_T)/2$, enters the second TOF arm containing MWPC2. The other combination of events in which the complementary heavier fragment $A_{\rm FFH} > (A_p + A_T)/2$ enters in this TOF arm were not analyzed because of some kinematic cuts imposed by the geometry of the detector setup.

The recoil velocity components of the composite system parallel $V_{||}$ and perpendicular $V_\perp$, to the beam, were determined from the measured folding angle and fragment velocities of each event, following the procedure given in Ref. [22], that is,

$$V_{||} = \frac{u_1 w_2 + u_2 w_1}{u_1 + u_2}, \tag{2}$$

and

$$V_\perp = \frac{u_1 u_2 \sin \Phi_{12}}{\sqrt{u_1^2 + u_2^2 - 2u_1 u_2 \cos \Phi_{12}}}, \tag{3}$$

where $u_i = v_i \sin\theta_i$, $w_i = v_i \cos\theta_i$, while v_i and θ_i are respectively, the velocities and the polar angles measured in the laboratory frame for the two fragments ($i = 1, 2$), and Φ_{12} is the azimuthal folding angle.

Binary fragmentation events arising from full momentum transfer are characterized by $V_{||}/V_{\rm CN} = 1$ and $V_\perp = 0$. As a typical example, Fig. 2 shows two-dimensional intensity

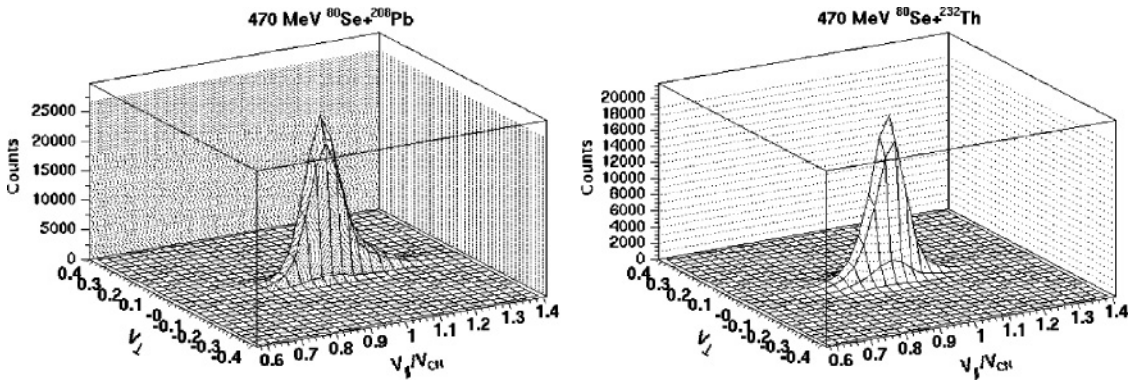

FIG. 2. Two-dimensional plots of counts vs $V_\perp$ and $V_{||}/V_{\rm CN}$ for both systems at $E_{\rm lab} = 470$ MeV.

plots with respect to $V_{||}/V_{CN}$ and $V_{\perp}$ of the fragments for the ^{80}Se+^{208}Pb and ^{80}Se+^{232}Th reactions at $E_{lab} = 470$ MeV. It is seen that the measured events are spread around $V_{||}/V_{CN} = 1$ and $V_{\perp} = 0$, as expected for the binary exit channels. A certain amount of tailing occurs on either side of the peak, which may be caused by energy straggling in the target and detector window, detector resolution, and contribution from transfer-induced fission. The binary events with full momentum transfer for each of the two systems were selected by gating the events with a window of $V_{||}/V_{CN} = 1.0 \pm 0.1$ and $V_{\perp} = 0.0 \pm 0.1$ to take into account the experimental resolution and the broadening of the fragment velocities due to sequential decay by neutron and charged-particle emission. For further analysis, the mass and total kinetic energy (TKE) of the fragments and neutron yields were determined for the events contained inside this gate.

IV. RESULTS AND DISCUSSION

A. Fragment mass and TKE correlations

Figure 3 shows the two-dimensional scatter plot of the counts vs fragment mass and TKE of the fragments for both systems at bombarding energies of 470 and 630 MeV, respectively, obtained after setting the gates on $V_{||}/V_{CN}$ and $V_{\perp}$ as discussed above. In the present analysis, only the class of events where the light fragments enter the TOF arm containing MWPC2 was analyzed, and the results presented here include a reflection of the experimental data around the mass of the symmetric splitting $A_{FF} = (A_P + A_T)/2$.

It is seen that the scatter plots are dominated by events close to target and projectile masses which correspond to deep inelastic collision (DIC) type of events. However, in the near-symmetric region, one observes two classes of events. For fragments with mass around 125, one class of events corresponding to the tail of the DIC events peaks around 180 MeV in TKE. For the other class of events presumably arising from deep quasifission (QF) and fusion fission (FF), the TKE distribution peaks at a higher energy around 230–250 MeV. It is observed that in both reactions around the symmetric mass, a significant number of events correspond to QF and FF. The polygonal gate covering near-symmetric events in each plot in Fig. 3 was visually marked to discriminate it from the tailing of the DIC branch and to select events corresponding to QF and FF at all bombarding energies**.** It can be seen from Fig. 3 that the contribution in the gated symmetric region is increasing with bombarding energy for both systems.

The mass distributions corresponding to the polygon gated region for both systems are shown in Fig. 4 at all bombarding energies. In both cases, the symmetric and asymmetric components are present in all mass distributions. It is seen that for this selected gate, the mass distributions for the ^{80}Se+^{208}Pb case have a more asymmetric character than those for ^{80}Se+^{232}Th. In Fig. 4, the light fragment masses corresponding to the

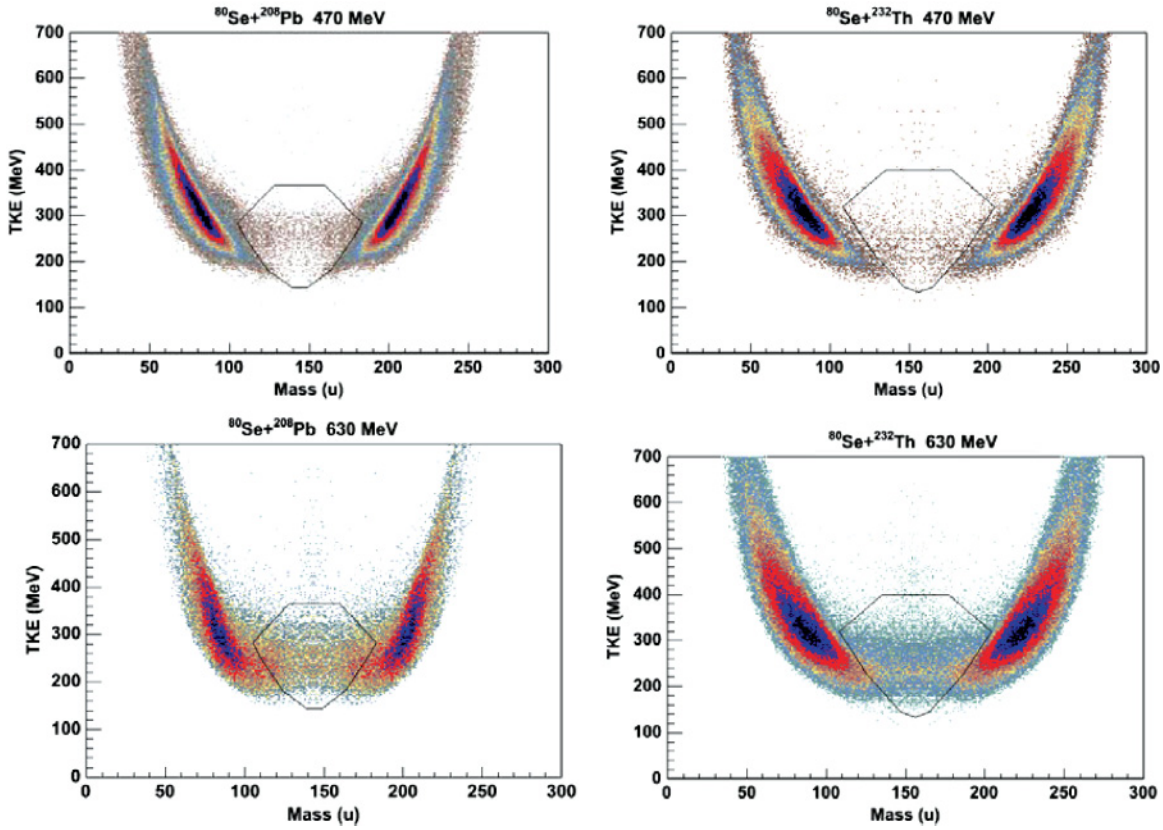

FIG. 3. (Color online) Mass-TKE scatter plot for binary events for ^{80}Se+^{208}Pb and ^{80}Se+^{232}Th systems at the bombarding energies of 470 and 630 MeV. The polygonal gate is used to select events around the symmetric region.

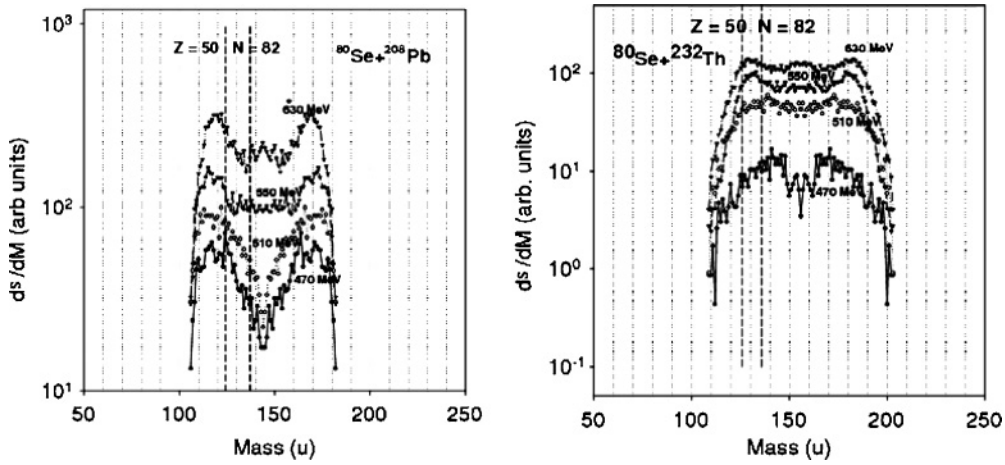

FIG. 4. Mass distributions (corresponding to the gated region in Fig. 3) for ^{80}Se+^{208}Pb and ^{80}Se+^{232}Th systems. The fragment masses corresponding to the expected shell closure at $Z = 50$ and $N = 82$ are indicated by dashed lines.

expected shell closures at $Z = 50$ and $N = 82$ are indicated by dashed lines as determined by knife cut. As we mentioned earlier and also as interpreted by Itkis *et al.* [23] for similar reactions involving heavy composite systems, the observed mass distributions can be ascribed to events arising from QF and FF reactions. In the present case of the ^{80}Se+^{232}Th reaction corresponding to larger Z_1Z_2 product, the QF component is expected to be larger. It is interesting to note that the symmetry region gets filled as the bombarding energy is increased in both systems, and the relative contribution in the symmetric region with respect to the mass-asymmetric component is larger in the ^{80}Se+^{232}Th system than in the ^{80}Se+^{208}Pb system.

Figure 5 shows the product of the center-of-mass bombarding energy and the relative cross section X_n of the fragments inside the gated region as a function of excess energy over the Coulomb barrier ($E_{\rm c.m} - V_B$) for both systems. The present bombarding energies are lower than the extra-extra-push energy needed for fusion in both cases in the static picture of Blocki *et al.* [14]. Therefore, there may be significant contribution to the observed yields in Figs. 4 and 5 from the deep QF process in addition to fusion-CN-fission (FF) process, as binary fragmentation may result from various stages during dynamic evolution toward CN formation after capture. On the other hand, if the fragment mass yield shown in Fig. 5 is largely due to the fusion process, then this may indicate that diffusion through the barrier, as pointed by Swiatecki *et al.* [12] plays an important role at higher temperatures to achieve fusion. As can be seen from the figure, the product of cross section for binary fragmentation and bombarding energy is higher for the ^{80}Se+^{208}Pb case than for ^{80}Se+^{232}Th at a given bombarding energy above the Coulomb barrier. Also, the increase in this product with bombarding energy is much less steep in the latter case. These features can be attributed to the higher extra-extra-push energy [11,12,14] required to form a compact configuration for fusion in the case of ^{80}Se+^{232}Th as compared to the ^{80}Se+^{208}Pb system, leading to smaller fusion-CN-fission in the former case. It will be interesting to compare these results with the predictions of dynamic model calculations which include the effects arising from the difference in the potential energy surfaces of the two systems where the flux through the symmetric and asymmetric valleys depends on the relative barrier (symmetric and asymmetric) heights [12].

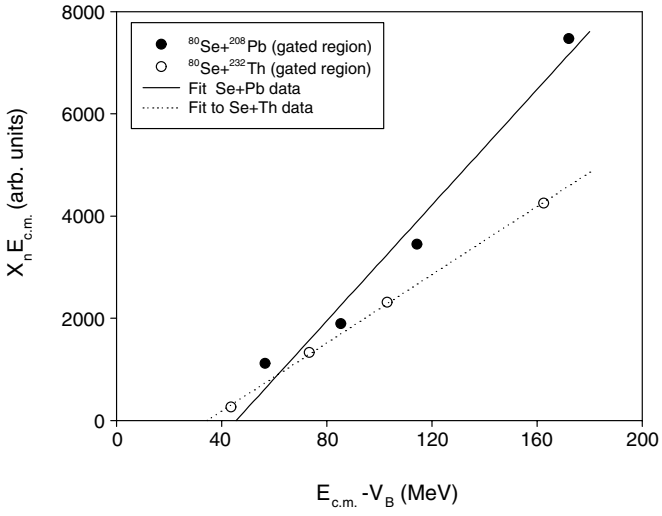

FIG. 5. Product of relative cross section and bombarding energy in center of mass of the near-symmetric events (gated region in Fig. 3) as a function of excess energy for both systems.

The average total kinetic energy of fragments for the fragment masses in the symmetric region is shown in Fig. 6 for various bombarding energies. It is seen that the average total kinetic energy remains nearly constant with bombarding energy within experimental uncertainties. For the ^{80}Se+^{208}Pb system, $\langle$TKE$\rangle = 255 \pm 12$ MeV, well in agreement with the expectation from Viola systematics [24]. This value is also agrees with our earlier measurement [19] for the ^{56}Fe+^{232}Th system which populates the same composite nucleus. For the ^{80}Se+^{232}Th system over the range of bombarding energies covered, $\langle$TKE$\rangle = 235 \pm 10$ MeV, which is significantly lower than that expected from the Viola systematics for compound nuclear fission and somewhat lower than the value of Itkis systematics [25] as shown in Fig. 6. The observation of

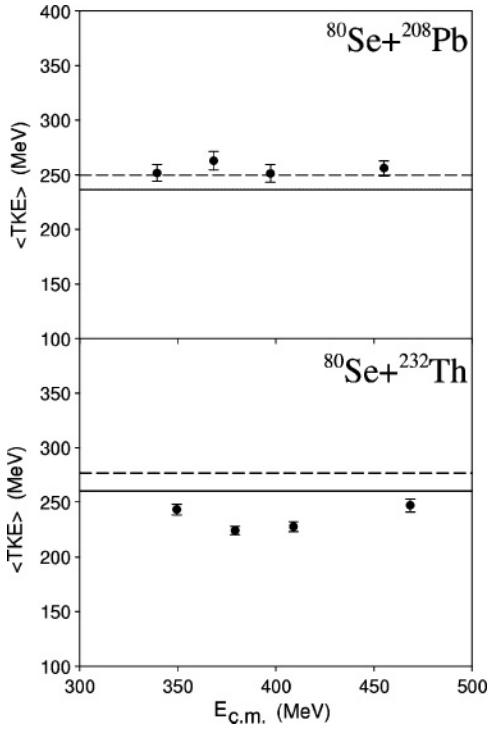

FIG. 6. Average TKE (for the symmetric masses) as a function of bombarding energy for both systems. Dashed and continuous lines correspond to the average TKE expected from Viola systematics $\langle \mathrm{TKE} \rangle = 0.1189\, Z^2/A^{1/3} + 7.3$ [24] and Itkis systematics $\langle \mathrm{TKE} \rangle = 0.104\, Z^2/A^{1/3} + 24.3$ [25], respectively.

a significantly lower TKE for the binary fragments in the ^{80}Se+^{232}Th reaction appears to indicate that in this case, there is a large admixture of QF events which also have a higher deformation of the scission configuration in the exit channel as compared to compound nuclear fission.

B. Fragment-neutron coincidences

The mass distributions for all selected binary-type events are shown in Fig. 7, with and without coincidence with neutrons for both systems at the different bombarding energies. Figure 7 also shows the approximate neutron yield as a function of the fragment mass as obtained by dividing the fragment-neutron coincidences by binary fragment yields, and correcting only for the geometric solid angle and detection efficiency of the neutron detectors. It may be noted that these neutron multiplicities are approximate, as they are not corrected for the angular correlation between the neutrons and the fragments, since the neutron spectra were too poor in statistics to perform a multisource deconvolution for all fragment masses. This fact also limited us in separating the pre- and post-fission components of the total neutron multiplicity.

As seen in Fig. 7, most of the neutron emission takes place from the near-symmetric mass region which is expected to be populated mainly by fusion-CN-fission and deep QF events. This hypothesis is justified by the fact that the fragments in the near-symmetric region seem to originate from a composite system which is almost fully relaxed not only in mass but also in energy during the collision process. This is also supported by the near independence of the measured TKE on the bombarding energy shown in Fig. 6.

The general trend of ν_{tot} increasing as the light fragment mass increases towards symmetry in both the systems is explained qualitatively by the expected increase of the available excitation energy as one moves towards mass-symmetric division. Also a larger available excitation energy in ^{80}Se+^{232}Th system as compared to the ^{80}Se+^{208}Pb system accounts for the higher observed yield of neutrons in the former case.

Figure 8 shows the average numbers of neutrons ν_{tot} corresponding to the symmetric mass bin as a function of the calculated compound nucleus excitation energy E_x^{CN}. These average numbers of neutrons ν_{tot} were determined after applying suitable corrections for the fragment-neutron correlations based on the estimated value of pre-scission neutron multiplicity for each case. These corrections were carried out as follows. The pre-scission neutrons for the symmetric region were simulated using the experimental E/A values and the fragment temperatures. The simulation was done employing the moving source model which has three neutron emitting sources, viz., the compound nucleus moving with a velocity V_{CN} and the two fragments whose velocities were taken from the experimentally determined values. The value of ν_{post} was fixed from the experimentally obtained number from our previous experiment for the ^{56}Fe +^{232} Th system [19], while systematics was used for the ^{80}Se+^{232}Th system [26]. The value of the pre-scission neutron multiplicity was determined in an iterative way to reproduce the experimentally observed fragment-neutron correlations. The compound nucleus excitation energy, E_x^{CN} is given by $E_x^{\mathrm{CN}} = E_{\mathrm{c.m.}} + Q_{\mathrm{CN}} = E_{\mathrm{c.m.}} + M_T + M_P - M_{\mathrm{CN}}$, where M_T and M_P are target and projectile masses and M_{CN} is the mass of the compound nucleus. It also follows that $E_x^{\mathrm{CN}} = E_{\mathrm{c.m.}} + Q_{\mathrm{CN}} = E_{\mathrm{c.m.}} - Q_F + Q_{\mathrm{gg}}$ where Q_F is the Q value for compound nucleus fission and Q_{gg} is the Q value for the exit channel with respect to initial target and projectile masses. Also, the value of Q_F is given by $Q_F = M_{\mathrm{CN}}$–M_{F1}–M_{F2}, where M_{F1} and M_{F2} are the masses of two fragments. E_x^{CN} was obtained by using the nuclear masses from Moller *et al.* [27] for the corresponding reactions wherein the compound nuclear masses ($M_{\mathrm{CN}} - A$) are given as 179.02 MeV for ^{288}116 and 257.42 MeV for ^{312}124.

Results from Fig. 8 can be compared with published data relative to superheavy composite systems having $Z > 100$, as populated in the earlier studies for the reactions of ^{64}Ni + ^{208}Pb, ^{238}U and ^{40}Ar + ^{208}Pb, ^{238}U [28]; ^{58}Ni, ^{64}Ni + ^{208}Pb [29]; and ^{48}Ca + ^{208}Pb, ^{238}U, ^{244}Pu, and ^{248}Cm [23]. Because of some differences in the nominal excitation energy of the populated compound nuclei, the experimental data are grouped in two different sets. The first includes the data on the ^{48}Ca induced reactions that are populating somewhat cold compound nuclei with excitation energies in the range $E_x = 33$–37 MeV. Data are shown in Fig. 9, where for the sake of comparison, average extrapolated values from Fig. 8 at $E_x = 35$ MeV are also reported. The results in Fig. 9 show that at the same compound nucleus excitation energy, there is a smooth increase of the total neutron multiplicity of

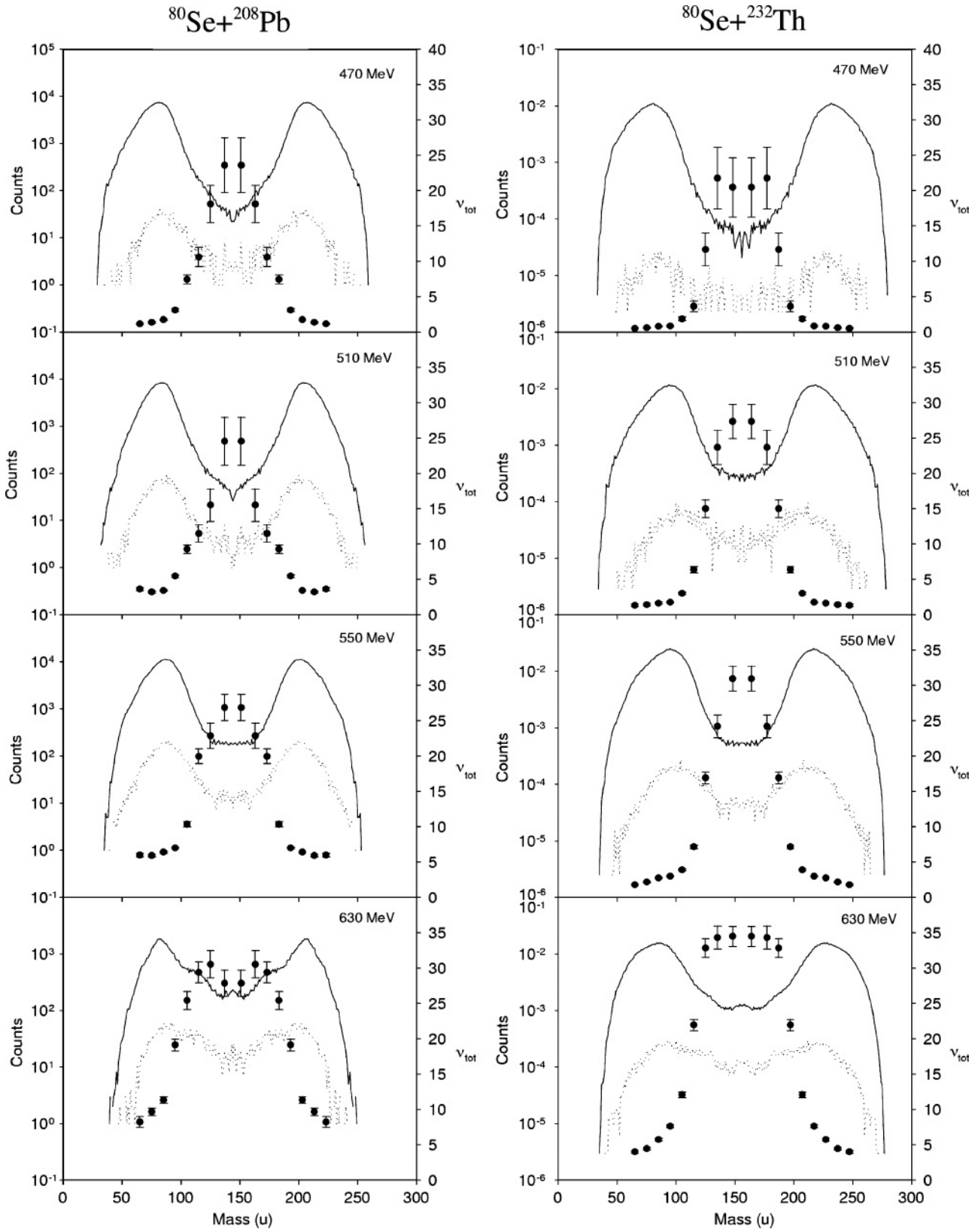

FIG. 7. Mass distributions of pure binary (solid line) and binary in coincidence with neutrons (dashed line). Total neutron multiplicities as a function of mass (solid points) were obtained by dividing the two distributions and correcting for neutron detection efficiencies.

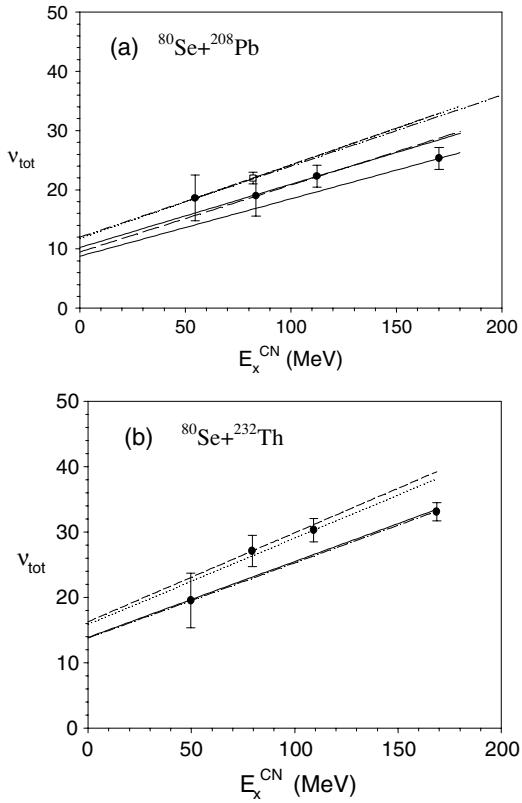

FIG. 8. ν_{tot} (after correcting for fragment-neutron correlations) as a function of compound nucleus excitation energy for ^{80}Se+^{208}Pb and ^{80}Se+^{232}Th. ν_{tot} for ^{56}Fe+^{232}Th from earlier work [19] is shown as an open square in (a). Lines correspond to energy cost for neutron emission.

about 0.6 neutron per unit of atomic number Z. A second group of data is shown in Fig. 10, where earlier measured neutron multiplicities are reported for $Z = 110$–124 and excitation energies in the range $E_x = 74$–85 MeV along with the results of the present work.

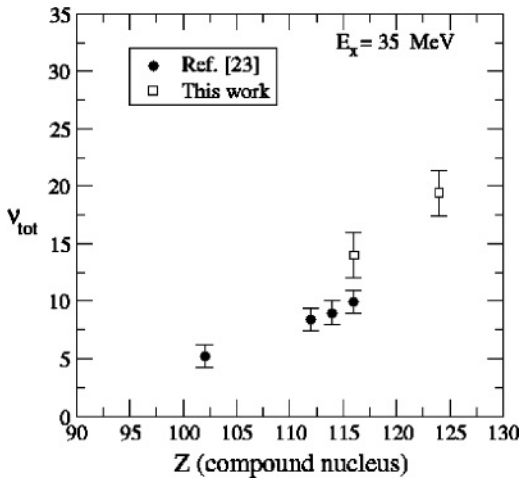

FIG. 9. Variation of ν_{tot} with atomic number of compound nucleus at the excitation energy of 35 MeV.

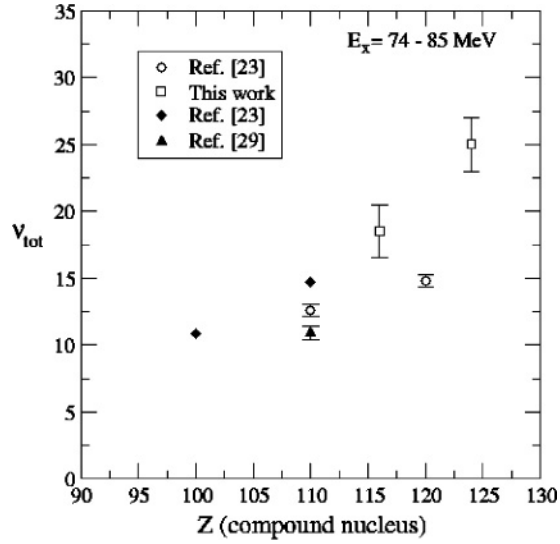

FIG. 10. Variation of ν_{tot} with atomic number of composite nucleus in the excitation energy range 74–85 MeV.

Also in this case, the general trend of the data shows a smooth increase of the neutron multiplicity of about 0.54 neutron per unit Z, which is not far from the value obtained for the lower excitation energy. These results are in line with the expected increase of $Q_{\rm eff} = Q_{\rm fiss} - \langle {\rm TKE} \rangle$ with the Z of the compound nucleus [26].

The lines drawn at each point of Fig. 8 correspond to the energy cost per neutron emission as calculated from the available energy, $E_{av} = E_{\rm c.m.} + Q_{gg} - \langle {\rm TKE} \rangle = E_x^{\rm CN} + Q_F - \langle {\rm TKE} \rangle$, and the total number of neutrons emitted corresponding to each data point. In this way, each data point is extrapolated to get an independent determination of ν_{tot} at zero excitation energy of the compound nucleus. In the case of ^{80}Se+^{232}Th, for calculating the energy cost per neutron emission, the value for $\langle$TKE$\rangle$ was taken from Viola's systematics, which is assumed to correspond to the case of compound nucleus fission of the hypothetical superheavy nucleus. For each system, all lines are seen to converge to some average value at zero compound nucleus excitation energy, which can be identified as the average number of neutrons emitted in the spontaneous fission (ν_{tot}^{sf}) of the corresponding hypothetical superheavy nucleus. The value of ν_{tot}^{sf} determined in this manner for the ^{80}Se+^{208}Pb system is $\nu_{tot}^{sf} = 10 \pm 2$, which is consistent with the value of 12±1 reported earlier by us [19] for the ^{56}Fe+^{232}Th system populating the same compound nucleus ^{288}116. The value of ν_{tot}^{sf} for the ^{80}Se+^{232}Th system corresponding to the superheavy compound nucleus ^{312}124 is obtained as $\nu_{tot}^{sf} = 15 \pm 2$, which is significantly large compared to other systems. It would therefore be of much interest to make measurements for still heavier systems to see if this trend continues.

V. SUMMARY AND CONCLUSIONS

The present work concerns the study of mass and TKE correlations and neutron multiplicities from binary

fragmentation of ^{80}Se+^{208}Pb and ^{80}Se+^{232}Th reactions that lead to superheavy composite systems of $(Z, A) = (116, 288)$ and (124, 312), respectively. The studies have been performed as a function of bombarding energy. The mass distributions in the near-symmetric region are distinctly different for the two systems, the former showing more asymmetry than to the latter.

The significant yield of events in the near-symmetric region for the heavy ^{80}Se+^{208}Pb and ^{80}Se+^{232}Th systems indicates that the diffusion mechanism plays an important role in heavy-ion reaction dynamics in the fusion path. The observed lower cross section of events in the near-symmetric region for the ^{80}Se+^{232}Th system with respect to the ^{80}Se+^{208}Pb at a given excess energy over the barrier, shows that the extra-extra-push energy needed for forcing the system for more compact shapes continues to be important in the diffusion mechanism. It is also noted that the average total kinetic energy of fragments for the ^{80}Se+^{232}Th system is significantly lower than the Viola's systematic value for compound nuclear fission, which may indicate more elongation for the scission shapes in the binary exit channel of such a heavy composite system. It may, however, be noted that the average TKE value for this system is closer to the systematics of Itkis [25]. The lower TKE value for the ^{80}Se+^{232}Th system is further confirmed by independent measurements of neutron multiplicities, where the neutron multiplicities are found to be significantly larger for the ^{80}Se+^{232}Th system than for the ^{80}Se+^{208}Pb system at comparable excitation energies. These results imply a significant contribution of deep quasifission events for the heavier ^{80}Se+^{232}Th system.

The measurement of $\nu_{\rm tot}$ as a function of compound nucleus excitation energy, $E_X^{\rm CN}$, enabled us to deduce the average number of neutrons expected to be emitted in the spontaneous fission of the two superheavy nuclei. The value of $\nu_{\rm tot}^{\rm sf}$ for spontaneous fission of $(Z, A) = (116, 288)$ and (124, 312) nuclei are estimated to be $\nu_{\rm tot}^{\rm sf} = 10 \pm 2$ and $\nu_{\rm tot}^{\rm sf} = 15 \pm 2$, respectively. The present results along with the earlier published data have revealed the systematic behavior of the increase in the average number of neutrons emitted in fission with Z of the compound nucleus at a given excitation energy.

[1] P. Armbuster, Acta Phys. Pol. B **34**, 1825 (2003).
[2] Yuri. Ts. Oganessian and Yuri. A. Lazarev, Heavy-ions and Nuclear Fission, Treatise in heavy-ion science, edited by D. A. Bromly, vol. 4.
[3] Akira Iwamato *et al*. Nucl. Phys. **A596**, 329 (1996).
[4] M. G. Itkis, Y. T. Oganessian, and V. I. Zagrebaev, Phys. Rev. C **65**, 044602 (2002).
[5] A. S. Zubov, G. G. Adamian, N. V. Antonenko, S. P. Ivanova, and W. Scheid, Phys. Rev. C **65**, 024308 (2002).
[6] M. G. Itkis *et al*., J. Nucl. Rad. Sci. **3**, 57 (2002).
[7] M. G. Itkis *et al*., Phys. At. Nucl. **66**, 1118 (2003).
[8] Yu. Oganessian *et al*., Nature (London) **400**, 242 (1999); Eur. Phys. J. A **15**, 201 (2002).
[9] D. J. Hinde *et al*., Phys. Rev. Lett. **89**, 282701 (2002).
[10] W. J. Swiatecki, Phys. Scr. **24**, 113 (1981).
[11] S. Bjornholm and W. J. Swiatecki, Nucl. Phys. **A391**, 471 (1982).
[12] W. J. Swiatecki, K. Siwek-Wilczynska, and J. Wilczynski, Phys. Rev. C **71**, 014602 (2005).
[13] Peter Moller and Arnold J. Sierk, Nature (London) **422**, 485 (2003); P. Moller *et al*., Nature (London) **409**, 785 (2001).
[14] J. P. Blocki *et al*., Nucl. Phys. **A459**, 145 (1986).
[15] Y. Aritomo and M. Ohta, Nucl. Phys. **A744**, 3 (2004).
[16] Y. Aritomo, T. Wada, M. Ohta, and Y. Abe, Phys. Rev. C **59**, 796 (1999); Y. Abe, Eur. Phys. J. A. **13**, 143 (2002).
[17] T. Materna *et al*., Nucl. Phys. **A734**, 184 (2004).
[18] see M. G. Itkis *et al*., Nucl. Phys. **A734**, 136 (2004), and references therein.
[19] P. K. Sahu *et al*., Phys. Rev. C **72**, 034604 (2005).
[20] A. Saxena *et al*., Phys. Rev. C **65**, 064601 (2002).
[21] A. Saxena *et al*., Nucl. Phys. **A730**, 299 (2004).
[22] E. Mordhorst *et al*., Phys. Rev. C **43**, 716 (1991).
[23] M. G. Itkis *et al*., Nucl. Phys. **A734**, 136 (2004).
[24] V. E. Viola, K. Kwiatkowski, and M. Walker, Phys. Rev. C **31**, 1550 (1985).
[25] M. G. Itkis and A. Y. Rusanov, Fiz. Elem. Chastits At. Yadra **29**, 389 (1998).
[26] D. Hilscher and H. Rossner, Ann. Phys. (Paris) **17**, 471 (1992).
[27] P. Moller *et al*., At. Data Nucl. Data Tables **59**, 185 (1995).
[28] D. J. Hinde, D. Hilscher, H. Rossner, B. Gebauer, M. Lehmann, and M. Wilpert, Phys. Rev. C **45**, 1229 (1992).
[29] L. Donadille *et al*., Nucl. Phys. **A656**, 259 (1999).